

# We are IntechOpen, the world's leading publisher of Open Access books Built by scientists, for scientists

4,800

Open access books available

122,000

International authors and editors

135M

Downloads

Our authors are among the

154

Countries delivered to

TOP 1%

most cited scientists

12.2%

Contributors from top 500 universities



WEB OF SCIENCE™

Selection of our books indexed in the Book Citation Index  
in Web of Science™ Core Collection (BKCI)

Interested in publishing with us?  
Contact [book.department@intechopen.com](mailto:book.department@intechopen.com)

Numbers displayed above are based on latest data collected.

For more information visit [www.intechopen.com](http://www.intechopen.com)



---

## How to Characterize Cylindrical Magnetic Nanowires

---

Fanny Béron, Marcos V. Puydinger dos Santos,  
Peterson G. de Carvalho, Karoline O. Moura,  
Luis C.C. Arzuza and Kleber R. Pirota

Additional information is available at the end of the chapter

<http://dx.doi.org/10.5772/63482>

---

### Abstract

Cylindrical magnetic nanowires made through the help of nanoporous alumina templates are being fabricated and characterized since the beginning of 2000. They are still actively investigated nowadays, mainly due to their various promising applications, ranging from high-density magnetic recording to high-frequency devices, passing by sensors, and biomedical applications. They also represent suitable systems in order to study the dimensionality effects on a given material. With time, the development in fabrication techniques allowed to increase the obtained nanowire complexity (controlled crystallinity, modulated composition and/or geometry, range of materials, etc.), while the improvements in nanomanipulation permitted to fabricate system based either on arrays or on single nanowires. On the other side, their increased complexity requires specific physical characterization methods, due to their particular features such as high anisotropy, small magnetic volume, dipolar interaction field between them, and interesting electronic properties. The aim of this chapter was to offer an ample overview of the magnetic, electric, and physical characterization techniques that are suitable for cylindrical magnetic nanowire investigation, of what is the specific care that one needs to take into account and which information will be extracted, with typical and varied examples.

**Keywords:** magnetic materials, nanotechnology, cylindrical magnetic nanowires, nanoporous alumina templates, characterization techniques

## 1. Introduction

The continuing progress in fabrication techniques nowadays lead scientists to succeed in producing nanosystems that are always smaller, more complex, and/or fabricated with more control. This achievement is highly interesting for both fundamental studies and technological improvements, since it provides novel systems permitting to test phenomena at mankind frontiers of knowledge. However, the counterpart is that these new nanosystems also require improvements in the characterization technique field, to yield more efficient, more sensible, and sometimes up to revolutionary, characterization methods. Without the ability to adequately probe the fabricated system characteristics, they remain useless and their promised advances need to wait until the development of suitable characterization techniques.

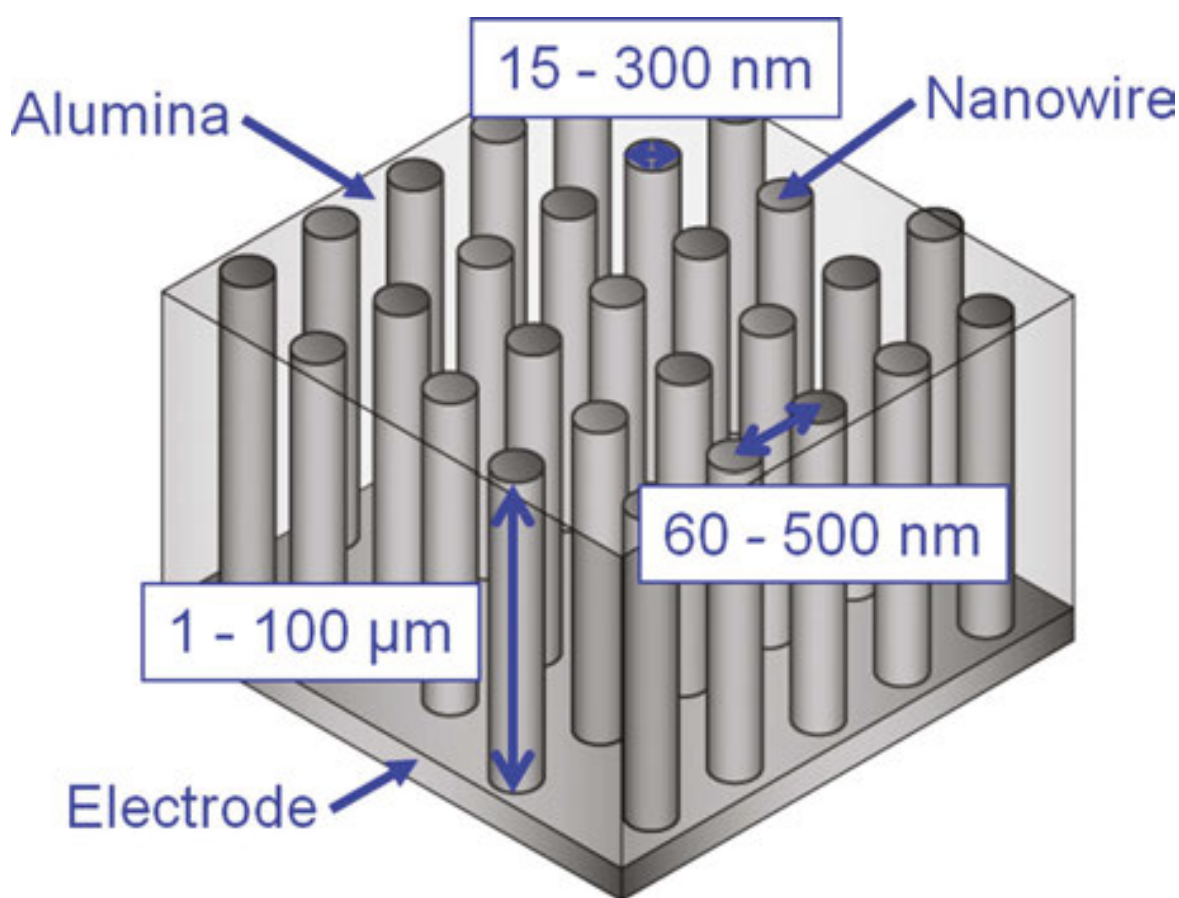


**Figure 1.** Representation of nanowire arrays embedded in a nanoporous alumina template. Reprinted with permission from [11]. Copyright 2010 by InTech.

Cylindrical magnetic nanowires represent a good example of the kind of nanosystems that become enabled due to a new fabrication technique. After the finding regarding how to obtain controlled nanoporous alumina templates by Masuda et al. in 1995 [1], the ordered, parallel, and with high-aspect ratio pores were quickly identified as perfect mold for electrodeposited metallic nanowires (**Figure 1**) [2–4]. Using magnetic materials, those nanowires are still actively

investigated nowadays, mainly due to their various promising applications, ranging from high-density magnetic recording [5] to high-frequency devices [6], passing by sensors [7], and biomedical applications [8]. They also represent suitable systems in order to study the dimensionality effects on a given material [9, 10]. With time, the development in fabrication techniques permitted to increase the obtained nanowire complexity (controlled crystallinity, modulated composition and/or geometry, range of materials, etc.), while the improvements in nanomanipulation permitted to fabricate systems based either on arrays or on single nanowires.

However, characterizing cylindrical magnetic nanowires presents specific challenges, due to their particular features. Among them, the small volume of a nanowire, and therefore its low magnetic signal, complicates both the manipulation of individual nanowires for their subsequent characterization and most of the single nanowire magnetic probing. It also limits the electrical current that a nanowire can support without melting, making them highly sensible to electrical discharge. Furthermore, nanowires present, by definition, a high-length/diameter ratio, typically larger than 50. This peculiar shape induces a mechanical fragility along the nanowire, thereby making its manipulation difficult and facilitating the apparition of longitudinal mechanical stress, which may interfere with their properties. From a magnetic point of view, this high-aspect ratio yields a large magnetic shape anisotropy that typically governs its magnetic behavior. Another important component influencing it is the large dipolar interaction field among nanowires when in array conformation, due to the small interdistance between them. However, this interaction field also needs to be taken into account when nanowires are free, like in solution. Finally, a last particular feature is the large nanowire surface (in comparison to its volume). It makes nanowires highly sensible to their environment, which may be an advantage, as in sensors, but can also be an issue while characterizing them (e.g., favoring the surface oxidation).

As previously stated, the magnetic nanowires' increased complexity requires specific characterizations, in order to efficiently understand their properties and behavior and take advantage of their novelty. The understanding of a magnetic system, such as magnetic nanowires, requires studying not only its magnetic behavior but also its electrical and physical properties. The emphasis on one or another aspect depends on the specific objective of the study or application. Therefore, the aim of this chapter is to offer an ample overview of the physical, electrical, and magnetic characterization techniques that are suitable for cylindrical magnetic nanowire investigation. For each method, the specific care that one needs to take into account and which information can be extracted are discussed, with typical and varied examples.

## 2. Physical characterization

Since magnetic properties are intrinsically linked to the system morphology, composition, and crystalline structure, they represent fundamental information while investigating magnetic nanowires. A common first step is to verify the obtained nanowire geometry by microscopy, either scanning electron microscopy (SEM) or transmission electron microscopy (TEM). Coupled to these microscopes, other spectroscopy techniques allow knowing the nanowire

composition, such as energy-dispersive X-ray spectroscopy (EDS) and electron energy loss spectroscopy (EELS). Radiation diffraction techniques yield information about the crystalline or magnetic structure and can be performed on the complete array, through X-ray, neutron, or electron diffraction, or locally on a nanowire section, with the help of a high-resolution TEM (HRTEM). Finally, phase transitions are well probed through specific heat measurements.

## 2.1. Geometry/morphology

As any nanostructure, nanowire fabrication often requires a visual inspection of the obtained product, before pursuing further characterization. Even if nanowires are basically long cylinders, their exact geometry (diameter, length, and interdistance in the array) directly influences their magnetic behavior. For example, their coercivity is highly sensible to their diameter, much more than to their length, while their interdistance controls the interaction field strength in the array, among others. Due to the fabrication technique used, nanowires grown in nanoporous alumina templates always exhibit a distribution, even very narrow, of their geometric parameter values. Furthermore, since nanowires are not restricted to homogeneous cylinders, their morphology also needs to be probed.

Such information can be obtained by electron microscopy techniques, due to the length scale required (less than 5-nm resolution at minimum). Scanning electron microscopy (SEM) and transmission electron microscopy (TEM) are the two best equipments for nanowire imaging. While the resolution of the first is lower, it is compensated by the facts that it is a cheaper, more widespread and easier to operate microscope.

### 2.1.1. Scanning electron microscopy (SEM)

SEM is a technique that enables the inspection of nanostructures by means of an electron beam guided through magnetic and electrostatic lenses. The wealth of different information that can be obtained by SEM method is caused by the multitude of signals that arise when an electron interacts with the specimen. The different types of electron scattering (backscattered, secondary, and Auger electrons) are the basis of most electron microscopy methods [12]. The widespread use of SEM became possible after 1958, when researchers from Cambridge (UK) built the first commercial prototype [13]. The typical primary electron beam used in a SEM is of 1–30 kV, with a beam current of 1 pA to 20 nA that can be focused in about 2–100-nm spot size, depending on the emitter source [14, 15]. A detailed description of the SEM operation can be found in [16].

This technique is highly adequate for proper measurements of the nanowire (and array) dimensions. Array cross-sectional view (easily obtained by simply breaking the fragile alumina template) facilitates the evaluation of geometrical parameter distribution (**Figure 2a**). Free nanowires can also be investigated, after selectively dissolving the alumina template and dispersing them on a substrate, generally Si (**Figure 2b**). Despite the relatively low resolution of SEM, it commonly allows zooming on some specific nanowire regions, such as the dendritic region at the bottom, if voltage reduction protocol described in [17] is used to thin the alumina barrier layer and allows the pores filling by electrodeposition (**Figure 2c**). Finally, the evalua-

tion of the pores-filling ratio can be completed by the top view of the array (**Figure 2d**). Additionally, as a non-destructive technique, one can inspect the nanowires along with electrical measurements, thermal annealing, or chemical reactions inside the SEM chamber [18]. However, electron beam exposure can induce hydrocarbon molecule deposition (from the vacuum chamber) on the scanned nanowire surface, leading to some contamination [19]. This can be avoided by reducing the beam current and exposure time over the surface [15].

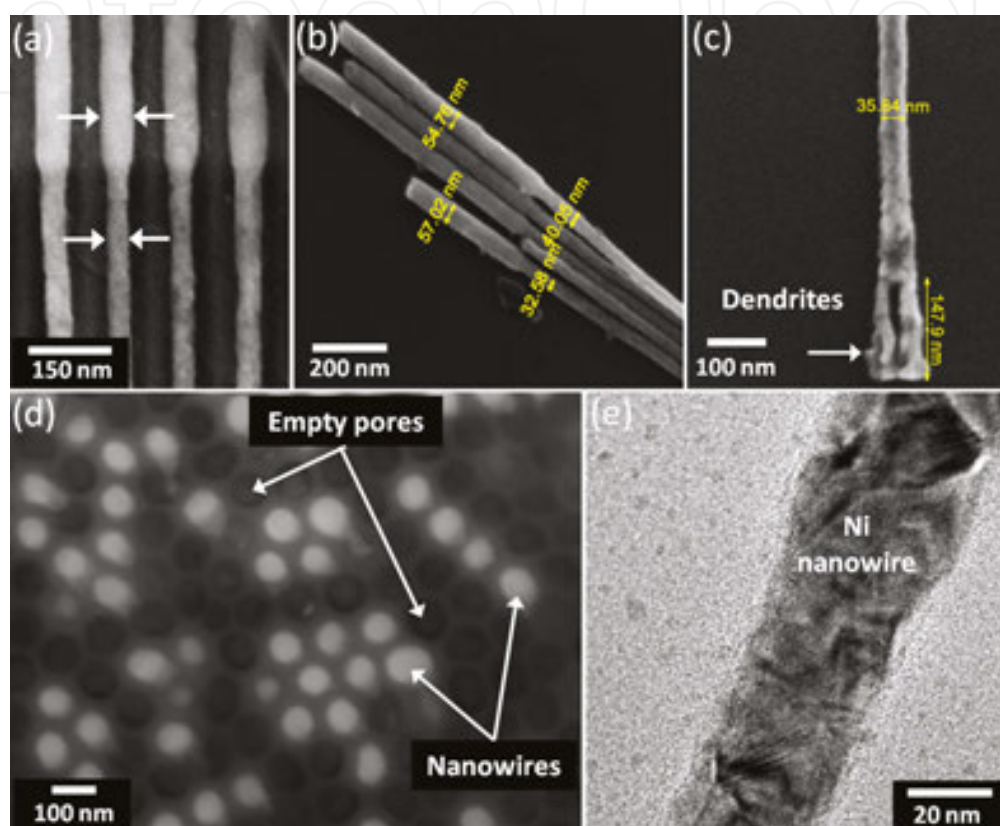


**Figure 2.** (a–d) SEM images of Ni nanowires with modulated diameter fabricated through the three-step anodization technique [20]. (a) Cross-sectional view, showing the diameter modification region; (b) zoom on free nanowires upper segment; (c) zoom on the dendritic region, at the nanowire base; (d) array-top view, where the filled pores appear clearer; and (e) TEM image of a Ni nanowire region. Reprinted with permission from [21]. Copyright 2015 by IEEE.

### 2.1.2. Transmission electron microscopy (TEM)

In order to observe the nanowires' geometrical aspects in more detail, higher resolution images can be obtained by using TEM. In a conventional TEM, a thin specimen is irradiated with an electron beam with uniform current density. Typically, the acceleration voltage is at least 100–200 kV, while medium voltage instruments work at 200–500 kV to provide better transmission, and some equipments can reach up to 3 MV. The use of such a high voltage allows to produce a very small electron beam spot (typically <5 nm and, at best, <0.1 nm in diameter). On the other hand, strong electron/atom interactions through elastic and inelastic scattering can lead to some damages to the sample. This technique therefore requires a very thin specimen,

typically of the order of 5–100 nm for 100-keV electrons, depending on the sample material [22, 23].

Fortunately, most nanowires are thin enough in order to be directly investigated by TEM, without further preparation than dispersing free nanowires on a carbon TEM grid. Interesting morphological information that can be obtained includes surface roughness, layer interface sharpness, or even atomic plane directions, to name a few, besides more precise geometrical characterization than with a SEM (**Figure 2e**). Generally, TEM nanowire characterization is not limited to geometry and morphology but specialized in local investigation. It usually takes advantage of the high-energy electron beam to perform local spectroscopy (Section 2.2). Moreover, given the small beam diameter, large electron diffraction occurs on the sample, which reveals useful crystallographic information that will be described more in detail in Section 2.3.2. Finally, even local magnetic information can be obtained, as will be discussed in Section 4.3.2. As expected, its operation presents much more difficulties compared to SEM.

A common challenge concerning the inspection by electron microscope of nanoporous alumina membrane is the charging effects from the electron beam on the scanned area (mainly insulating). This effect can be avoided by depositing a very thin layer (<50 nm) of carbon or metal on the top surface [12, 24], whereas the dimensions of the inspected structures are larger than the metal layer thickness. However, the SEM contrast of nonconductive specimens varies widely depending on the coating metal and thickness, which influences the measurement's accuracy on the scanned structures [25]. For TEM analysis, if the charge dissipation is insufficient, as is the case for insulating materials, the sample becomes unstable under the beam and the analysis becomes impossible.

## 2.2. Chemical composition

Since chemical composition is not necessarily totally controlled during the nanowire fabrication, either by electrodeposition or other alumina template-filling methods, probing their chemical composition is essential. This is especially important for alloyed or multi-element nanowires, as well as for multilayered ones. In the last case, a direct visualization of the chemical composition configuration is highly helpful. This is also true for local investigation, such as for surface oxidation, for example.

Therefore, it is highly advantageous to use some features of the electron microscopes described above to simultaneously perform a composition characterization of the nanowires. Mainly, both SEM and TEM possess a high-energy electron beam, which allows high sensibility, while their scanning possibilities permit to map the chemical composition, usually superimposed to their morphology image. The typical techniques used for nanowires are the energy-dispersive X-ray spectroscopy (EDS) and the electron energy loss spectroscopy (EELS). Generally speaking, while the first determines the presence or not of an element, the second can probe their chemical environment. Both techniques can lead to a mapping of local chemical properties with high spatial resolution when coupled to a TEM, whereas EDS can also be performed in a SEM chamber.

### 2.2.1. Energy dispersive X-ray spectroscopy (EDS)

EDS measures the energy and intensity distribution of the X-rays generated by the impact of the high-energy electron beam on the surface of the sample (**Figure 3a**). The principle is based on the inner-shell electrons that may be excited by the incident beam, thus leaving holes in the atom's electronic shells. When these holes are filled by higher energy electrons, the energy level difference creates a released X-ray. Since its energy depends on the electronic structure of the atom, the elemental composition within the probed area can be determined to a high degree of precision. More information about the EDS technique is available in [26].

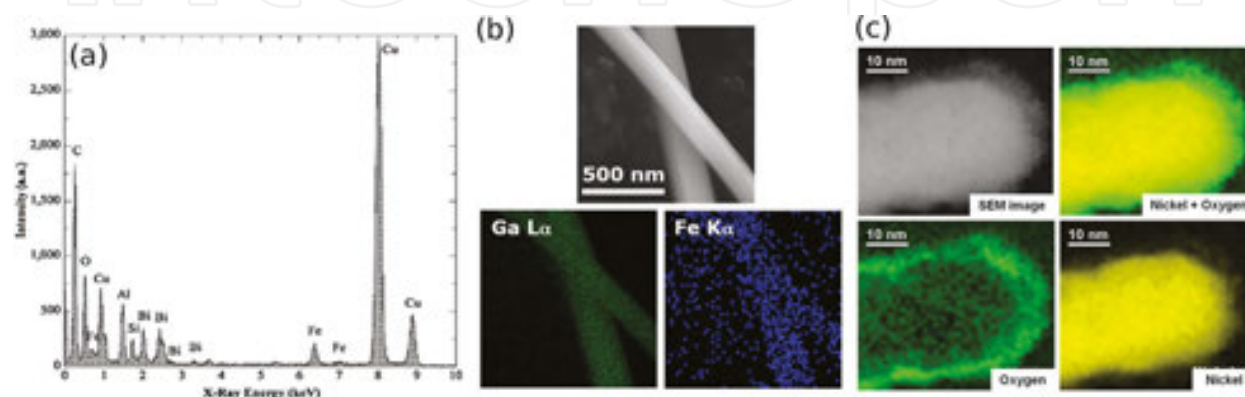


**Figure 3.** (a) EDS spectrum of BiFeO<sub>3</sub> nanowires made by sol-gel preparation into alumina template. Reprinted with permission from [10]. Copyright 2013 by Elsevier Ltd, (b) EDS composition mapping of Fe<sub>3</sub>Ga<sub>4</sub> nanowires fabricated through the metallic-flux nanonucleation method. Reprinted with permission from [9]. Copyright 2016 by Nature Publishing Group, and (c) EELS analysis for the composition mapping of Ni nanowire after dissolving the alumina template. Reprinted with permission from [28]. Copyright 2013 by Brazilian Microelectronics Society.

Specifically in nanowire characterization case, EDS is particularly useful to determine their chemical composition [27], their stoichiometry, and their impurity content. As mentioned before, since EDS is a local probe, it allows focusing on the nanowires, being either free or still in the alumina array (viewed in cross section). On counterpart, EDS data from nanowires require to be analyzed keeping in mind the low material thickness. Especially for light elements, the incident electron beam may not sufficiently interact with the atoms while passing through the nanowire diameter, thus preventing the emission of the characteristic X-ray spectrum of the material. In these cases, elemental percentage cannot be determined with precision, and EDS results are limited to probe the presence or not of the elements (in concentration above the detection limit). Care should also be taken about the EDS mapping spatial resolution (**Figure 3b**). Since it depends on the size of the interaction volume, which in turn is controlled by the accelerating voltage and the mean atomic number of the sample, the spatial resolution is better while performing EDS mapping in a TEM than in a SEM, on the order of 0.5 and 10 nm, respectively.

### 2.2.2. Electron energy loss spectroscopy (EELS)

In order to overcome the EDS disadvantages and obtain more precise information about the material chemical composition, one can use EELS technique instead. It allows obtaining



chemical information with a better energy resolution, passing from tens of eV for EDS to around 1 eV for EELS. Moreover, the EELS spatial resolution is generally higher than the corresponding EDS experiment because the EDS data are affected by beam broadening, unless the sample is very thin [29]. However, as a main drawback, EELS represents a more difficult technique to operate.

During an EELS measurement, some incident electrons of known energy will be scattered through inelastic interactions. The detection of the energy and momentum of the scattered electrons provides information on the excitations in the sample. As in EDS, inner-shell ionizations allow to determine the material atomic composition. However, a careful analysis of the spectrum also gives access to data about the chemical environment, such as the chemical bonding and the valence-/conduction-band electronic properties, among others [30, 31]. Since EELS is based on energy losses, the spectrum identification is facilitated for sharp and well-defined excitation edges, such as exhibited by low atomic number elements. The reader interested by more information about EELS as surface analysis technique is referenced to [32].

Therefore, in addition to determine the atomic composition for nanowires including light elements, EELS nanowire characterization is commonly used to investigate their oxidation state. In this case, the EELS- and TEM-coupled results can show the nanowire surface oxidation after being released from the alumina template (**Figure 3c**), which is critical for good electrical contact, as will be explained in Section 3.2. Another EELS capacity especially useful for nanowires is the ability to locally determine the valence state of a given element in the nanowire.

### 2.3. Structural characterization

Nanowires are by definition highly anisotropic, due to their elongated shape. However, in addition to the induced large axial shape anisotropy, one may need to also consider the magnetocrystalline contribution to the effective anisotropy. Therefore, the crystalline texture is especially important to resolve for nanowires made of materials with non-negligible magnetocrystalline anisotropy, like Co in hexagonal-close package (hcp). In this case, the uniaxial magnetocrystalline anisotropy constant being of the same order of magnitude than the shape anisotropy of an infinite cylinder, it makes the effective anisotropy very sensitive to the nanowire texture.

Crystalline structure being, by definition, a repetitive pattern of a unit cell of atoms, the characterization techniques are based on the diffraction principle. X-ray diffraction (XRD) is the most common one and can be applied to nanowires. However, due to their small volume, the measurements require to be performed on several nanowires together, preventing to resolve local modifications of the crystalline structure along the nanowires. Substituting the incident beam from X-rays to high-energy electrons, precise local crystalline structure can be probed. Therefore, TEM chamber, through techniques such as selected area electron diffraction (SAED) and high-resolution TEM, represents an ideal environment for nanowire crystalline structure investigation.

### 2.3.1. X-ray diffraction (XRD)

As mentioned above, monochromatic X-rays are used in XRD technique as incident beam that will be scattered through elastic interactions with the atom electrons. For some specific scattering angles that depend on the crystalline structure, a constructive interference is obtained and detected. Careful analysis of the diffraction pattern yields the identification of the crystal symmetry and unit cell, as well as allowing characterization of more subtle aspects, such as stress and disorder in the unit cell.

X-ray diffraction is commonly used to determine the basic composition, crystalline phase, and texture of electrodeposited nanowires. Due to geometry restrictions, the XRD experiment is usually performed in the  $\theta$ - $2\theta$  mode with the scattering vector parallel to the nanowires inside the porous template, but it is also possible to remove the nanowires from the template and dispose them on a surface (such as a silicon wafer or glass) to set the scattering vector perpendicular to the nanowires. In the first geometry, only the crystalline planes perpendicular to the scattering vector contribute to the diffractogram peaks (**Figure 4a**). This particular situation yields that, besides the usual element and phase determination through their position, their relative intensity gives information about the crystalline texture, that is, the preferential grain orientation in the nanowires [33]. The XRD rocking curve technique, where the detector angle is fixed and the sample slightly tilted around a given angle, is a more powerful tool for the nanowire crystalline texture determination [34] (**Figure 4a** inset). However, due to the small volume of the electrodeposited nanowires and because they often do not completely fill the pore length, the diffractogram count can be very low and additional diffraction peaks arising from the template/substrate complicate the data analysis. Therefore, synchrotron radiation is preferred, since it leads to a higher signal coming from the nanowires.

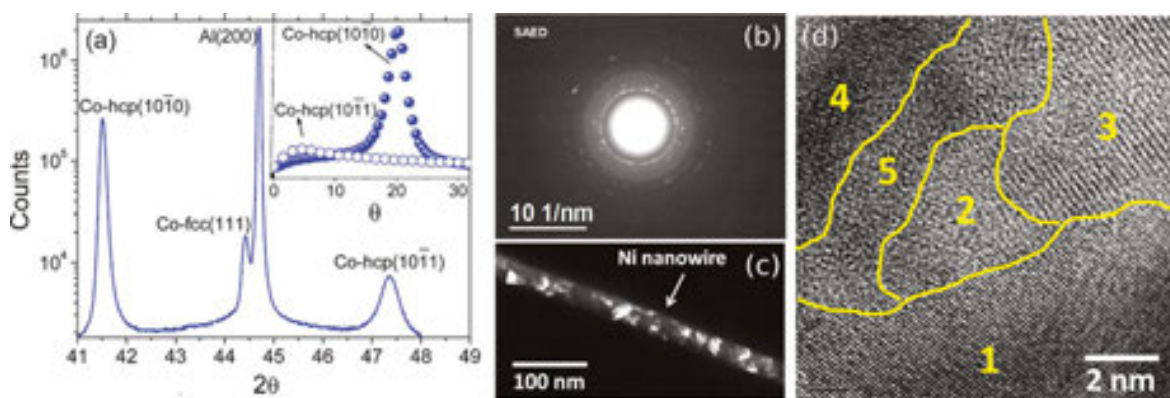


**Figure 4.** (a) XRD pattern of hcp/fcc bi-crystalline Co nanowires. Inset: rocking curves for two different hcp peaks. Reprinted with permission from [34]. Copyright 2015 by AIP Publishing LLC. (b–d) Structural characterization through electron diffraction of a polycrystalline Ni nanowire. Reprinted with permission from [21]. Copyright 2015 by IEEE, (b) SAED diffraction pattern, (c) dark-field TEM images, showing size distribution of planes under the same diffraction condition, and (d) HRTEM showing the crystallographic planes.

### 2.3.2. Electron diffraction

Another way to improve the nanowire diffraction signal is to again take advantage of the incident high-energy electron beam present in a TEM. The diffraction principle remains similar as in XRD, with the difference that it is electrons that are elastically scattered, allowing a higher resolution. Also, the diffraction is probed in transmission, instead as in reflection, yielding a pattern of bright spots indicating the constructive interference conditions. Several probing techniques are available in a TEM chamber, but due to their morphology (thin but long) and nanoscale dimensions, nanowires represent an ideal system for those.

One can perform a selected area electron diffraction (SAED) in a region as small as of a few hundreds of nanometers, which can be a specific region along a nanowire. Indexing the obtained diffraction pattern is a powerful tool to study its crystalline structure (**Figure 4b**). The very short electron wavelength (of the pm order, but with relatively low energy when compared with X-rays) gives access to a precise description of the atom's position. Additionally, one can also select a diffraction spot of SAED and enhance the contrast of the volume that contributes to that spot (**Figure 4c**). This imaging technique, called dark-field TEM, is useful to investigate planar defects, stacking faults, and grain size along individual nanowires, quickly allowing identifying repetitive crystalline pattern. Additionally, direct atomic observation is possible through a high-resolution TEM (HRTEM), to image the crystalline planes (**Figure 4d**). Therefore, by directly measuring the interplanar distances, one can determine the phase and orientation of the grains, and also estimate their size. For a brief review of SAED and HRTEM applied to nanowires, one can refer to [35].

Finally, it is noteworthy to mention that specific heat, a technique which will be explained in the next section, can also be used to indirectly investigate nanowire crystalline structure [9]. The measurement does not require removing the nanowires from the template, which can represent a great advantage. On the counterpart, one requires a bulk sample of the same material, in a crystalline structure thought as similar as in the nanowires. Specific heat measurement yields the system Debye temperature, which is related to the phonon spectrum. By comparing the Debye temperatures, it is possible to see if both phonon spectra, and therefore crystalline structures, are similar or not.

## 2.4. Phase transition

In certain systems, it is advantageous to explore their physical properties by means of specific heat measurements. The specific heat of a material is one of the most important thermodynamic properties denoting its heat retention or loss of capacity. Therefore, its variation with temperature or magnetic field may indicate crystalline and/or magnetic phase transitions [36]. The specific heat acquisition can be performed in a small-mass calorimeter. In one of the various measurement protocols, it is placed into the sample chamber which controls the heat added to/removed from a sample while monitoring the resulting change in temperature. During a measurement, a given quantity of heat is first applied at constant power for a fixed time, before allowing the sample to cool down during an equivalent time. Unlike other techniques that monitor magnetic transition phase, such as magnetometry, specific heat measurements can

provide important additional information on the electronic structure and crystal lattice. However, care to the extent and in the analysis of the results need to be made more cautiously.

Like bulk systems, nanowires can undergo phase transitions. Interestingly, the transition temperature and nature may be modified for nanowires, as consequences of their lower dimensionality [9, 37] (**Figure 5**). However, performing specific heat measurements on nanowires represents a challenging task, due to the requirements to remove the contributions to the signal arising from everything else than the nanowires with precision. For nanowire arrays, this means to also measure, in the same conditions, a similar (in mass and geometry) empty alumina template. Accuracy in results depends on the correct mass determination of each component, which needs to be estimated for the nanowires.

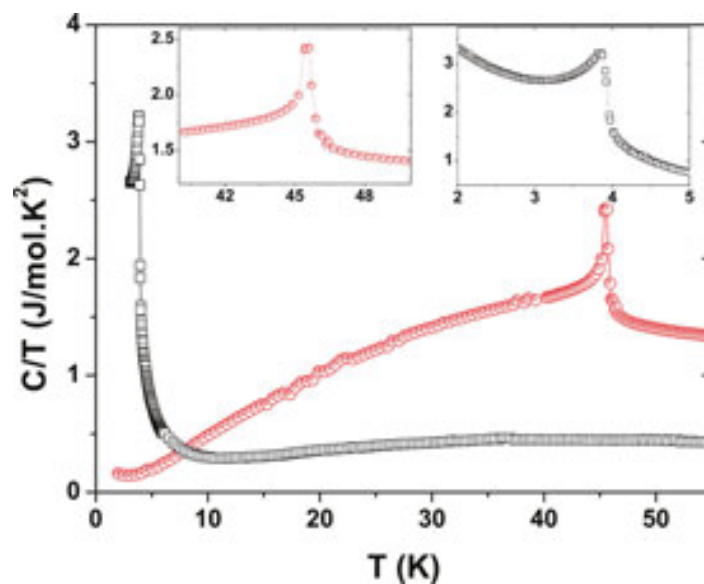


**Figure 5.** Specific heat divided by temperature as a function of temperature of  $\text{GdIn}_3$  nanowires (black curve) and its bulk correspondent (red curve), fabricated through the metallic-flux nanonucleation method. The sharp peaks show an antiferromagnetic transition, zoomed in the respective inset. Reprinted with permission from [37]. Copyright 2014 by Elsevier Ltd.

### 3. Electrical characterization

The growing interest in magnetic nanowires is connected to the possibility of employing them for advanced applications in wide technological fields. For example, nanowires represent ideal candidates for sensor devices, since they present high sensitivity to their environment [38, 39]. Moreover, they are presently intensively investigated for a large range of spintronic devices, due to the nanowire dimensions comparable or smaller than scaling lengths in magnetism and spin-polarized transport. Transport and magnetic properties, such as anisotropic magnetoresistance, field-induced magnetization reversal in single nanowires, domain-wall magnetoresistance, quantized spin transport in nanoconstrictions, among others

[40–43], represent essential characterization for nanowires intended to play a major role in tomorrow's high technology.

In this chapter, we focus on direct current (DC) electrical characterization. The reader interested in radio-frequency (RF) nanowire measurements is referred to [6]. The main difficulty to perform electrical measurements on nanowires is to succeed in obtaining a good electrical contact. In this sense, several techniques have been implemented [38–40]. Here, we will restrain ourselves to the description of electrical characterization performed on single or few cylindrical nanowires. First, we describe a technique where the connected nanowires remain inside the nanowire array, thereby feeling the interaction field from their neighbors. In the second part, a method to measure free single nanowires is presented.

### 3.1. Nanowires embedded in array

Electrical characterization of nanowire arrays still embedded in porous alumina is an interesting technique because of their spatial ordering. In this case, the idea is to electrically connect nanowires both extremity, which is facilitated by the electrode already present at the nanowires' bottom, used for their electrodeposition. Even if the barrier layer thinning method can be used to obtain an electrical contact [44], removing completely the barrier layer and closing the pores with a thick conductive film (usually Au) is preferred to lower the resistance. The top contact may be fabricated by filling the remaining pores length by a metallic material, like Cu [41, 43], or by mechanically polishing the top of the template before depositing an electrode by sputtering [40, 42].

Using lithography techniques, one can limit the template region electrically connected, measuring current transport over thousands of nanowires at the same time. The main advantage of this technique is to improve signal-to-noise ratio. In counterpart, the electrical characteristic in response to an electrical excitation is averaged [41], which prevents spin-transfer experiments.

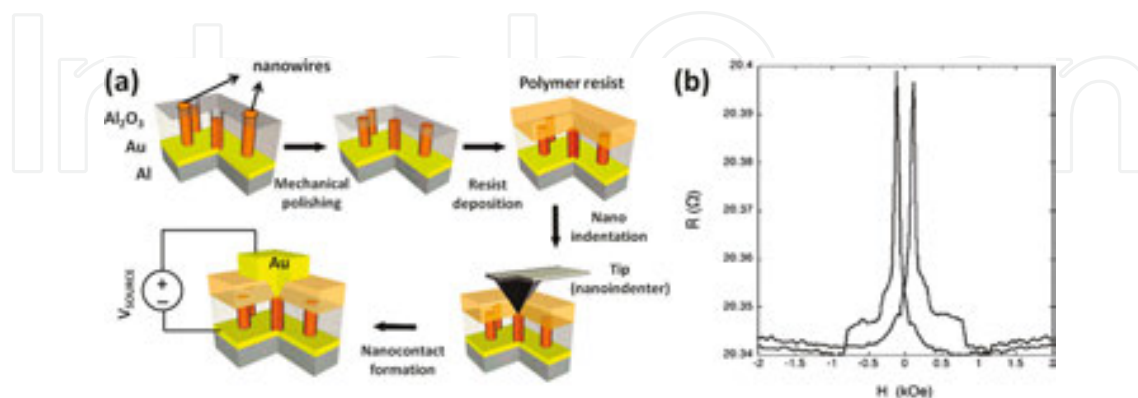


**Figure 6.** (a) Schematic illustration of the single nanowire contacting process on an array of nanowires electrodeposited in supported nanoporous alumina template and (b) magnetoresistance curve for Py/Cu/Py spin-valve nanowire with 80 nm of diameter and external magnetic field in-plane with the membrane. Reprinted with permission from [40]. Copyright 2007 by American Chemical Society.

However, one can also define electrical nanocontacts on a single electrodeposited nanowire inside the porous membrane. This can be done by the indentation of an ultrathin-insulating photoresist layer deposited on the top face of the thinned alumina template after the electrodeposition. A modified atomic force microscope designed for local resistance measurement is used as a nanoindenter, allowing an easy access point onto individual nanowires at the surface of the template [40, 42], as shown in **Figure 6a**. As a consequence, magnetic properties, such as magnetoresistance signal, can be extracted from one individual nanowire (**Figure 6b**).

Despite the presence of the interaction field on the measured nanowire, this technique presents several advantages. First, the template size and shape yield a convenient sample-handling method [41]. Second, since the probed nanowire remains inside the alumina template, it does not suffer surface oxidation due to the contact with alumina-etching solution and ambient atmosphere. The major drawback of this oxidation is that it increases the nanowire resistance. As a consequence, it makes spin-transfer experiments more difficult, leading to a small giant magnetoresistance signal. Moreover, it favors the apparition of heating problem due to Joule effect, limiting the current density that one can inject in the nanowire before melting it.

### 3.2. Free nanowires

To avoid magnetic interactions between closer nanowires inside the porous membrane, which can influence the electrical and magnetic measurements of a single nanowire, one can release them from the membrane using a convenient etching solution. Two options exist to establish an electrical contact on a single nanowire, both involving the design of proper electrodes by optical or e-beam lithography. The first one consists of patterning the electrodes after dispersing the nanowires on a substrate [45]. While this method does not require nanowire manipulation, the critical step is the careful electrode alignment with the lying nanowire. Here, we will focus on the opposite technique, where the electrodes are first patterned and the free nanowires are placed afterwards between them. Depending on the nanowire manipulation technique, this method can reach large outflow.

For metallic nanowires, dielectrophoresis (DEP) technique allows to adequately position the nanowires to electrically connect them with the electrodes to further transport measurements. After chemically etching the alumina membrane, the nanowires must then be dispersed in dimethylformamide (DMF), a dielectric medium, in order to avoid nanowire cluster formation [21, 38, 41, 43]. Then, the metallic nanowires suspended in the DMF can be directly manipulated through alternating electric fields produced by a pair of electrodes separated by a gap region, as reported in [38] (**Figure 7a**). For optimized DEP parameters, one can trap one single nanowire to carry out electrical/magnetic measurements [38, 39, 41, 43] (**Figure 7b**).

As shown, DEP is an adequate tool to insert nanowire between electrodes for electrical transport measurements [38]. As already mentioned above, compared to the in-template electrical measurement, this technique removes the effects from the dipolar field from neighboring nanowires. Moreover, it permits to use a four-point resistance measurement method, since the electrode geometry is more versatile. Therefore, it makes possible to pattern a series of electrodes on a single nanowire in order to follow a domain-wall propagation. However, when the nanowire touches the electrodes, a large contact resistance is sometimes

present due to native oxide or organic residues, leading to a Schottky-like behavior (nonlinear). Several options are available to reduce the contact resistance, such as depositing a thin metallic layer on the nanowire extremities by focused ion beam-induced deposition (FIBID) (**Figure 7c**) [38]. Another option consists of improving the contact resistance by passing a low current into the nanowire, allowing subsequent temperature-dependent electrical resistivity and magnetoresistance measurements (**Figure 7d**) [28].

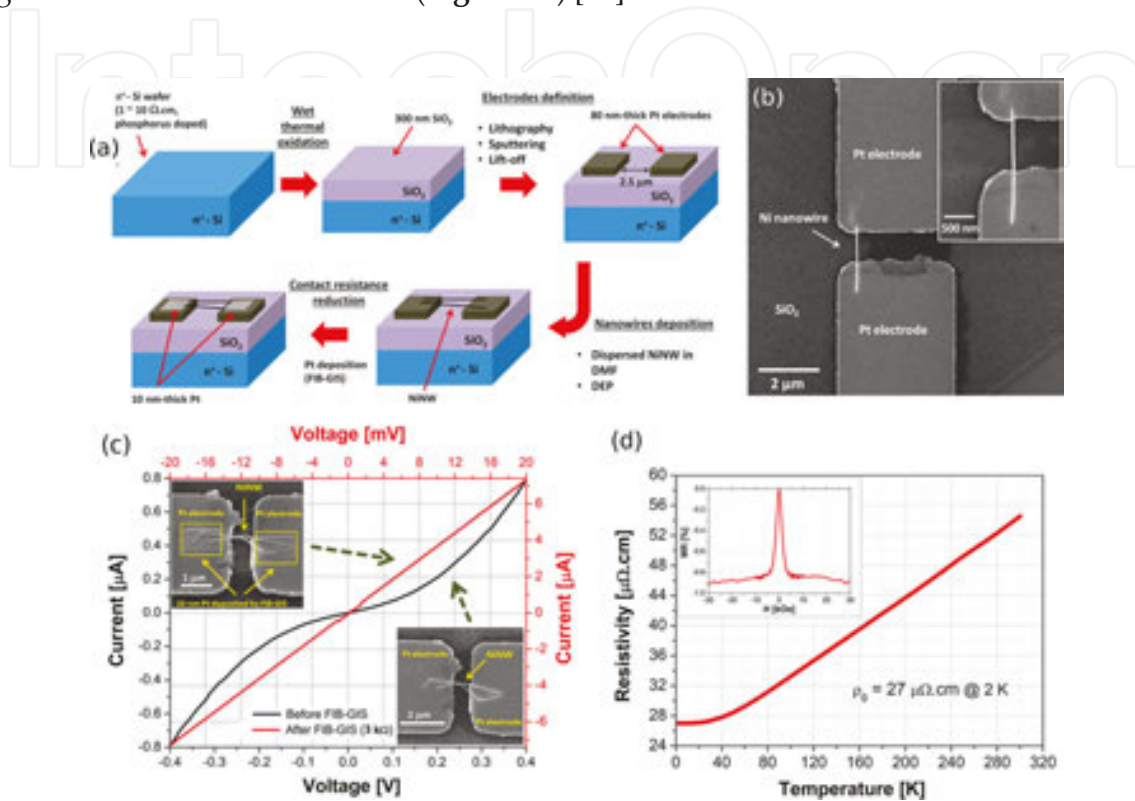


**Figure 7.** Electrical characterization of free Ni nanowires manipulated through DEP technique, as presented in [38]. (a) Schematic illustration of the sample preparation, (b) SEM image of one single nanowire deposited on electrodes, (c) current versus voltage curves before (black, left, and down axes) and after (red, right, and up axes) 10-nm-thick Pt layer deposition by FIBID (a and c reprinted with permission from [38]. Copyright 2015 by American Vacuum Society), and (d) resistivity evolution with temperature of one single nanowire, showing metallic behavior. Inset: magnetoresistance measurement with the current flowing perpendicular to the applied field at 300 K. Reprinted with permission from [28]. Copyright 2013 by Brazilian Microelectronics Society.

Whatever the techniques used to connect a single nanowire, its electrical characterization is subjected to a special care about the current that can flow through it. Above a certain limit, it begins to damage the nanowire due to heat dissipation. Therefore, in addition to control the current during the electrical measurements, one needs to also prevent electrical discharge when preparing the sample.

#### 4. Magnetic characterization

Obviously, the investigation of magnetic nanowires cannot be complete without probing their magnetic properties. Magnetometry, which is the magnetization measurement, yields the basic

magnetic behavior, typically through the acquisition of a major hysteresis curve. For an array, it can be performed on a vibrating sample magnetometer (VSM) or a superconducting quantum interference device (SQUID), while micro-SQUID and magneto-optical Kerr effect (MOKE) are suitable for single nanowire. All these magnetization measurement techniques can also be used to perform specific field routine, such as first-order reversal curves (FORCs), which give the statistical distribution of hysteresis operators, or the angular dependence, to probe the magnetization-reversal processes. On the other hand, useful magnetic characterization is not limited to the magnetization value acquisition. Nanowire array magnetization reversal can be probed by means of magnetic force microscopy (MFM), while imaging the domain walls and/or magnetic structure along a single nanowire is enabled by MFM and electron holography, for example. For its part, ferromagnetic resonance (FMR) is an adequate tool to probe the material anisotropy.

#### 4.1. Magnetometry techniques

While typical nanowire arrays exhibit a magnetic signal relatively easy to measure with conventional equipment, due to the high nanowire density, single nanowires require more sensible technique. Furthermore, the sample manipulation does not present specific challenge for measuring an array, apart from the magnetic field orientation with respect to the nanowire axis. However, the first problem to overcome before measuring single nanowire magnetization is their proper positioning. These differences naturally divide the magnetometry techniques between the array and single nanowire-oriented ones.

##### 4.1.1. Array magnetometry

Most of conventional magnetometers coupled with magnets able to apply field of at least 1 T are sufficient to measure the magnetization arising from a nanowire array. Due to the high density of nanowires, its magnetic signal typically yields several  $\mu\text{emu}$ , which is higher than the sensibility of standard magnetometer for bulk systems. The two main equipment used for nanowire magnetic characterization are the vibrating sample magnetometer (VSM) and the superconducting quantum interference device (SQUID) magnetometer. Both are based on Faraday's law principle, which states that a variation in the magnetic flux density passing through a conductive coil induces a current in this coil to compensate the variation. The sample is therefore magnetized by an external magnetic field and its position with respect to the detecting coils is changed, thus inducing a measured voltage that is subsequently converted in magnetic moment.

The VSM detection system [46] is simpler than the one in a SQUID. The sensing coils are usually copper coils located around the sample. A relatively good sensitivity is gained by mechanically vibrating the sample at a given frequency (typically less than 100 Hz) and using a lock-in amplifier to filter the signal induced. In counterpart, the SQUID benefits of a higher sensitivity. Here, the detector is a superconducting loop, which imposes a quantization of the magnetic flux. This loop contains two Josephson junctions that break the flowing current symmetry in the presence of a magnetic flux variation. For more information about SQUID operation, the reader is referred to the study of Ramasamy et al. [47].



Apart from the proper sample centering, nanowire array magnetization acquisition is relatively straightforward. The only experimental aspect to take care is the applied magnetic field direction relative to the nanowire axis, due to the anisotropy of the system (**Figure 8a**). Since the measurement is performed on a whole array, one needs to remember that it exhibits the array magnetic properties, which may differ from the individual nanowire ones (see Section 4.2.1). For example, the coercivity obtained represents when half of the array magnetic volume reversed its magnetization, while the susceptibility is related to the interaction field between the nanowires.

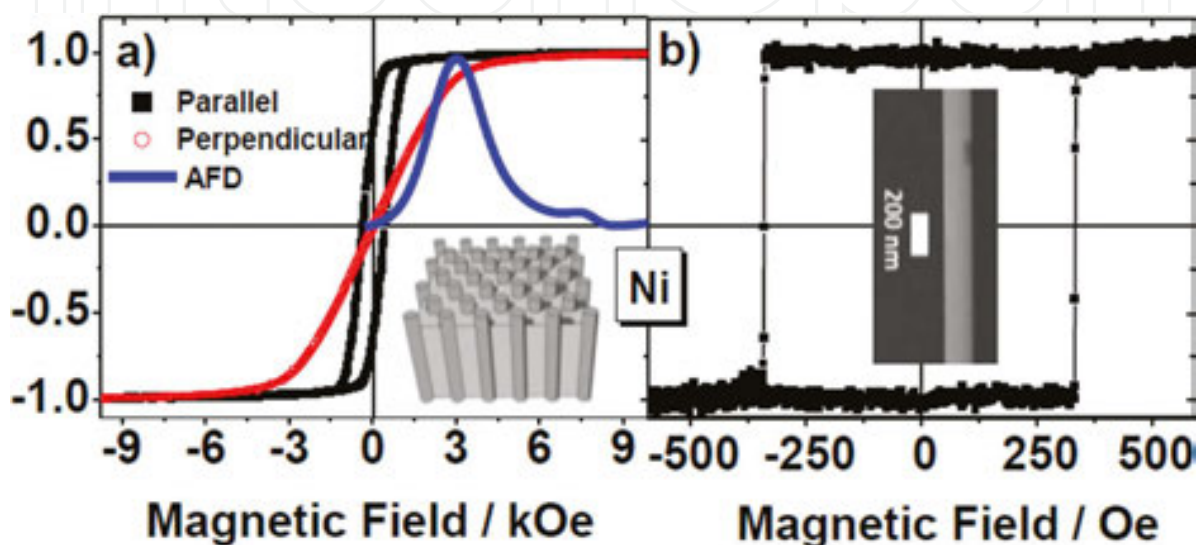


**Figure 8.** Typical normalized magnetization curves for Ni nanowires (130 nm of diameter,  $\approx 20\text{-}\mu\text{m}$  long). (a) Nanowire array measured both parallel (black) and perpendicular (red) to the nanowire axis on a commercial VSM. It evidences the axial easy axis of the array. In blue, the anisotropy field distribution calculated according to [48] and (b) single nanowire measured axially on a MOKE setup. The squared hysteresis loop denotes a clear axial easy axis. Reprinted with permission from [49]. Copyright 2012 by IOP Publishing Ltd.

#### 4.1.2. Single nanowire magnetometry

To overcome this discrepancy, the direct magnetic measurement of one nanowire should deliver the individual properties. However, in addition to the difficulties created by the necessity to adequately position the individual nanowire with respect to the sensing element, the low magnetic signal arising from a single nanowire represents a complex challenge. Two different solutions have essentially been implemented.

The first one consists of fabricating a micro-SQUID detector around a free nanowire lying on a substrate [50]. The nanowire proximity with the superconducting loop, coupled to its high-detection sensibility, allows performing magnetization measurement. However, this technique has several drawbacks that explain why it is not largely widespread. Mainly, the micro-SQUID detector fabrication, made by complex lithography, is restrained to a unique nanowire, thus severely limiting the number of single nanowires that can be characterized in a reasonable period of time.

On the other side, the magneto-optical Kerr effect (MOKE) is normally used as a superficial magnetic characterization technique due to its small penetration length. Nevertheless, its penetration length of the order of the tens of nanometer is enough to probe the magnetic signal from single nanowires, while actually removing unwanted background signal, as from the substrate. Compared to the micro-SQUID, the MOKE technique is advantaged by the facts that it can be performed on a conventional MOKE setup and allows to quickly measure several nanowires, making distribution properties possible to evaluate. It consists of shining an incident polarized light on the magnetic sample and measuring the rotation of the reflected light [51]. This rotation depends on the relative orientation of the incident polarization with the sample magnetization. Therefore, there exist three different configurations (longitudinal, transversal, and polar) that allow detecting magnetization in the parallel, perpendicular, and out-of-plane directions, respectively.

In order to succeed in measuring the magnetic properties of isolated nanowires by MOKE, it is important to carefully perform the measurement. Good focus of the laser spot on the sample and cautious alignment of the lens system are primordial to avoid signal loss. Additionally, the low magnetic signal requires that the hysteresis loops must be averaged several times (up to thousands) to improve the signal-to-noise ratio. As already stated, the magnetic characterization of single nanowires yields fundamental properties such as the individual switching field and squareness of nanowires [49] (**Figure 8b**). This information is essential to study the magnetization-reversal mechanisms in nanowires.

## 4.2. Magnetometry routines

Even if major magnetization hysteresis curves, from an array or a single nanowire, give a valuable characterization, the knowledge directly extracted from them remains limited: saturation magnetization, susceptibility, coercivity, squareness, and so on. However, different magnetic behaviors can be easily probed, still using the same setups as for the major curve acquisition. The idea consists of modifying the measurement routine in order to select a specific kind of behavior to follow and investigate. For example, instead of sweeping the magnetic field between saturation values, but performing reversal curves, which begin in the hysteresis area, one is able to get access to the switching of individual nanowires while measuring the whole array. This technique, called first-order reversal curve (FORC), is very powerful when applied to nanowire systems. Another possibility is to change the angle during the measurement, since nanowire magnetic behavior depends on their anisotropy. This technique represents an effective way to achieve to experimentally study the magnetization-reversal mechanisms occurring in the nanowires. Both procedures are easily implemented in any magnetometer and can be applied to both nanowire array and single nanowire. Therefore, they should be considered as part as basic nanowire characterization, along with major hysteresis curves, due to the richness of information obtained.

### 4.2.1. First-order reversal curve (FORC) technique

Major hysteresis curves yield the magnetic properties of whole nanowire arrays. However, the magnetization of the array can be viewed as the average of the nanowire magnetization. The

objective of the FORC technique is to extract the individual magnetic entities characteristics while performing a measurement on the whole system. A complete description of the implementation of the FORC method for nanowire arrays is available in [11]. It is based on the classical Preisach model, where magnetic entities are modeled as squared hysteresis operators called mathematical hysterons. In order to obtain the statistical distribution of these operators, only described by their width and field shift, Mayergoyz developed a specific field-sweeping routine [52]. It consists of minor curves beginning at a reversal field (inside the hysteretic area) and returning to the saturation (**Figure 9a**). The FORC result is calculated from these data through a second-order mixed derivative and represented as a contour plot (**Figure 9b**). If the measured system meets the required conditions for the classical Preisach model, it can be considered as the hysterons statistical distribution.

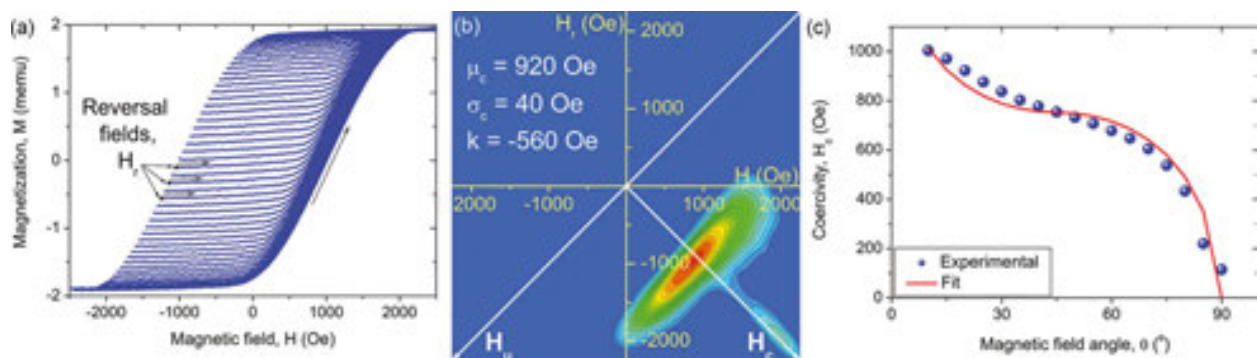


**Figure 9.** Different magnetization measurement procedure results applied to an Ni nanowire array (35-nm diameter, 3.5- $\mu\text{m}$  long). (a) First-order reversal curves measurement along the nanowire axis, (b) respective FORC result. Color scale ranging from blue (null value) to red (maximum value), and (c) angular evolution of the array coercivity along with the analytic fit for a transverse domain-wall nucleation. The effective anisotropy constant was evaluated at  $3.612 \times 10^5 \text{ erg/cm}^3$ .

Several nanowires, due to their large shape anisotropy, exhibit a squared hysteresis curves when measured axially. Therefore, the hysterons could be associated with the individual nanowire magnetic behavior, leading to a clever way to get access to the single nanowire properties without requiring to remove them from the template. This explains why the FORC technique is highly suitable to investigate nanowires. However, like most of real systems, nanowire arrays do not meet the criteria for the classical Preisach model, due to their interaction field. The FORC result analysis thus necessitates to be performed carefully. The physical analysis model, based on simulated behavior of physically meaningful hysterons, has been developed in this sense [53]. It allowed obtaining a quantitative parametrization of the FORC result in order to extract the mean and distribution width coercivity and the interaction field at saturation, among other values [54]. Even if the method is based on hysteretic operators, information about the system reversibility can also be extracted [55].

Typical axial FORC result for nanowire appears as a distribution narrow along the coercivity, while elongated along the interaction field axis (**Figure 9b**). It may be interpreted as nanowires with similar coercivity, and therefore geometrical dimensions, submitted to a large and almost uniform interaction field dependent on the magnetization. In general, a ridge may appear

along the coercivity axis and is attributed to the nonuniformity of this interaction field, the measurement being carried on a finite array [56]. In addition to the homogeneous nanowires, the FORC method remains suitable for more complex systems, such as multilayer nanowires, when coupled to the physical analysis model for the result analysis.

#### 4.2.2. *Angular-dependent magnetization curves*

From a general point of view, all anisotropic system behavior is highly dependent on the applied magnetic field direction. From the other side, varying the field angle allows obtaining data from which additional information may be extracted. On most of magnetometers working with an electromagnet, which produces a horizontal applied field, modifying the measurement angle is easy and generally implemented in the control software. It is more challenging for superconducting coil, since the magnetic field is vertical in this case. Manual angle variation is usually required, thus increasing the total measurement time.

For nanowires, the classical case is to perform hysteresis curves along the axial and transverse directions, to determine the easy axis direction (e.g., see **Figure 8a**). In the last years, angle-dependent magnetization curves turned out to be richer in information, after it proved its ability to be interpreted as a signature of the magnetization-reversal processes. Nanowires with diameter up to few hundreds of nanometers usually reverse their magnetization through the domain-wall nucleation/propagation mechanism. Depending on their properties, the domain wall nucleated may be either transverse or vortex. Assuming that a transverse domain-wall nucleation can be modeled as the coherent rotation of a volume equivalent to the domain wall [57], the angular nanowire coercivity can be calculated in this case [58] (**Figure 9c**). Deviations from this model can be interpreted as the occurrence of other mechanisms (curling, fanning, coherent rotation, etc.) or domain-wall types (mainly vortex), while fitting yields quantitative values of the anisotropy constants. A special care with the precision of the field direction angle should be taken during the measurement, but can be easily overcome while performing the analytical fit.

### 4.3. Magnetization imaging

For nanowires, the interest in obtaining a direct or an indirect visualization of their magnetic structure depends on the resolution and area observed. High-resolution imaging allows probing a particular region of the nanowire and observes details of the magnetic domains and domain walls, which is probably the best way to understand and to control them. Since the domain-wall dynamics is very sensitive to their morphology [59, 60], it is fundamental to know their geometry for all applications involving domain-wall propagation. The domain pattern of a whole nanowire, for its part, gives valuable information about its magnetization-reversal mechanism. Finally, investigations of the nanowire array complex magnetization reversal and interaction field are helped by large-scale imaging of several nanowires, usually performed on the template top surface.

The two last cases are well resolved by using the magnetic force microscopy (MFM) technique, where a magnetized atomic force microscopy tip maps the stray field. For further local

magnetic information, several methods have been developed. They are usually more complicated to operate than MFM and not always suitable for cylindrical nanowires, due to their geometry. Here, we focus on a powerful characterization that can be performed in a TEM chamber and that can yield highly valuable local information: electron holography.

The main problem concerning magnetization imaging of nanowires and nanowire arrays is that both systems are tridimensional, instead of planar. Therefore, one needs to keep in mind that the observation made is not complete and that some additional features of the internal magnetization structure may be hidden from the observer. By example, assumptions about the nanowire magnetic structure are required when imaging nanowire array top extremity. Also, the nanowires' cylindrical shape makes the domain-wall internal structure very difficult to be seen, like the core of a vortex domain wall, since it lays parallel to the nanowire axis and near its center.

#### 4.3.1. Magnetic force microscopy (MFM)

Among several techniques, the MFM is probably one of the most used magnetic imaging tools. Here, we give a brief description of the technique, but a most complete, although compact description, can be found in [61]. As mentioned above, the MFM is an atomic force microscope

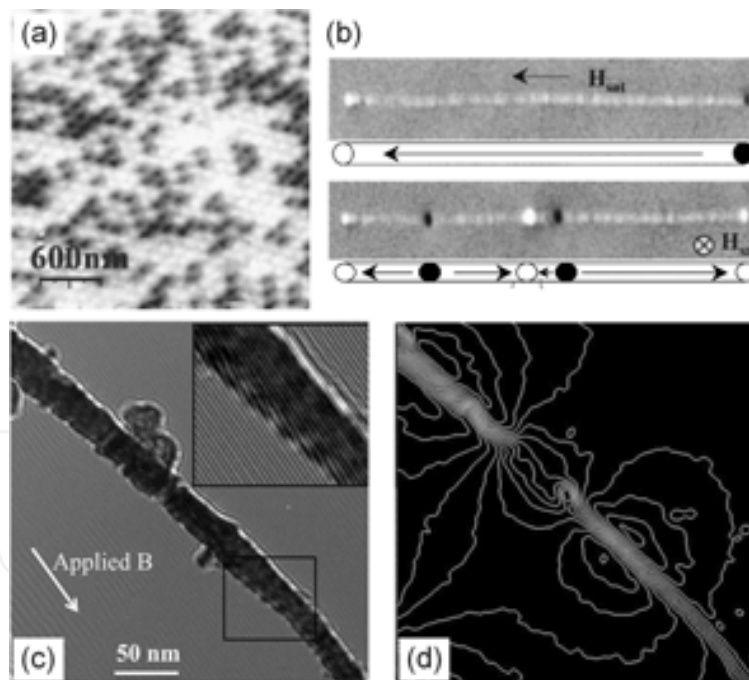


**Figure 10.** (a and b) MFM images in the remanent state. The clear and dark spots denoted outgoing and ingoing stray field, respectively. (a) Top surface of Ni nanowire arrays. The clear and dark circles represent the nanowires magnetized upward and downward. Reprinted with permission from [65]. Copyright 2004 by EDP Sciences, (b) individual 35-nm Co nanowire after saturation in a field parallel (top) and perpendicular (bottom) to the nanowire axis. A sketch of the possible domain pattern is underneath. Reprinted with permission from [64]. Copyright 2000 by American Physical Society, and (c and d) electron holography results of a multilayer Cu/CoFeB nanowire (80/230 nm) for an axial-applied magnetic field. Reprinted with permission from [66]. Copyright 2014 by AIP Publishing LLC. (c) Hologram. (d) Associated map of perpendicular magnetic field, with 0.1-T contour spacing.

with a magnetic tip, usually a thin (<50 nm) coated film with high coercivity of Ni, Co, or CoCr, among others, for the tip magnetization to be fixed during the scan. The tip lies on one end of a cantilever that raster scans the sample. The scanned area can be as large as 200  $\mu\text{m}^2$  and the typical resolution is 30 nm. In alternating current (AC) mode, which provides a better resolution, the cantilever tip is put to oscillate near its resonance frequency by piezoelectric crystals, while the tip-sample interaction changes the amplitude, frequency, and phase of the oscillating cantilever. All these changes are measurable (by a laser reflected from the cantilever) and can be used to calculate the force exerted at the tip by the sample. To consider only the magneto-static interaction between the tip and the stray field generated by the sample, the lift-height technique is usually employed. In this mode, the tip is brought very close to the sample and a first scan is performed. The tip is then lifted and a second scan is done, thus eliminating the topographic contribution. A lift height of 50 nm is usually sufficient to image nanowires. Due to the complicated and not necessarily fixed magnetization tip and the unsolvable problem of the reconstruction of the magnetization sample by the sensed sample stray field, MFM is usually considered as a qualitative technique. Despite this, it is very useful, especially if combined with other techniques such as magnetometry, magnetoresistance measurements, and micromagnetic simulations.

Since the samples do not require any special preparations, only to lay on a plane surface, MFM is used to image both the top of nanowire arrays and free nanowires. Due to the large axial shape anisotropy, nanowires are usually taken to remain monodomain under axial-applied magnetic field. Therefore, investigations about individual nanowire-switching field and complex magnetostatic interaction between nanowires take advantages of the large template area that MFM can scan [62, 63] (**Figure 10a**). Actually, this monodomain state can be directly observed by performing MFM imaging of free nanowires. It allows visualizing the magnetic domains along the nanowire, and thus the presence of domain walls [64] (**Figure 10b**). However, in cylindrical nanowires, the domain-wall length is typically of a few nanometers, for Co, Ni, Fe, and alloys. Therefore, the MFM resolution does not normally provide much information about the domain-wall geometry, especially if it is a vortex or a helical, that have a small stray field compared with transverse domain wall.

#### 4.3.2. *Electron holography*

Electron holography, performed in a TEM chamber, allows obtaining higher resolution imaging of the magnetic structure. The principle is to get access to the phase shift of the electron wave that traveled through the sample, not only to its amplitude, as in conventional TEM imaging techniques. By creating two paths for the electron beam, one passing through the sample while the other remaining undisturbed, the interference pattern creates an electron hologram, which depends on the phase shift. Therefore, the sample local magnetic properties influence the electron wave when passing through it and can be directly observed afterwards. More information about this powerful technique can be found in [67, 68], the second being specifically dedicated to magnetic material investigations.

Being performed using the high-energy electron beam from a TEM, typical electron holography resolution is of 5 nm and results are usually associated with micromagnetic simulations.

Due to the technique complexity, the best use of electron holography for nanowires is to probe the fine magnetic structure that is out of range for MFM equipment. More specifically, it allows to obtain a clear image of nanowire domain walls [69], as well as the detailed domain pattern created by multilayers [66] (**Figure 10c and d**).

#### 4.4. Anisotropy probing

Finally, as was mentioned several times, nanowire magnetic behavior is intrinsically related to their anisotropy, both global and local variations. Even if magnetometry can be used to indirectly probe the system anisotropy properties, ferromagnetic resonance (FMR) is a powerful technique to obtain more accurate data. The FMR phenomenon is based on the resonance arising when the frequency of an applied transverse AC magnetic field is equal to the material Larmor frequency, which is the frequency of magnetization precession around the effective magnetic field. Since the anisotropy energy modifies the effective magnetic field, even the anisotropy constant distribution is accessible through FMR. A complete description of the phenomenon and the various ways to measure it is reviewed in [70].

**Figure 11.** (a) Resonance field evolution with the magnetic field angle for CoFeB, Ni, and Ni/Cu nanowires. Reprinted with permission from [74]. Copyright 2007 by AIP Publishing LLC and (b) illustration of the double-resonance phenomenon occurring in a CoFeB nanowire array (40-nm diameter, 200- $\mu\text{m}$  long). Left: schematic of the microstrip line and major hysteresis curve branch used to measure FMR. Right: resulting contour plot. Reprinted with permission from [72]. Copyright 2009 by AIP Publishing LLC.

In the specific case of monodomain nanowires, both the anisotropy intensity and direction distributions are highly important since electrodeposited nanowires generally present homogeneities, which could greatly affect their magnetic behavior. On the other side, electromagnetic wave propagation directly depends on the medium effective anisotropy, leading to a crucial information for all nanowire applications related with high-frequency devices (**Figure 11a**) [71]. Finally, the array magnetization reversal may lead to the interesting phenomenon of

double resonance (**Figure 11b**) [72]. Several setups have been developed to measure FMR in nanowires and nanowire arrays. The reader interested to push further his knowledge in the area is referenced to the following book chapter [73].

## 5. Conclusion

In summary, the adequate use of the different characterization techniques available is essential for any researcher that is investigating magnetic nanowires, since the cost in time and money is high. Moreover, improper data analysis can lead to incorrect conclusions, while the unknown existence of a characterization technique can severely delay the advancement of a research project. This chapter is meant to serve as a reference guide for the specific system that constitutes magnetic nanowires.

## Author details

Fanny Béron\*, Marcos V. Puydinger dos Santos, Peterson G. de Carvalho, Karoline O. Moura, Luis C.C. Arzuza and Kleber R. Pirola

\*Address all correspondence to: [fberon@ifi.unicamp.br](mailto:fberon@ifi.unicamp.br)

Gleb Wataghin Physics Institute, State University of Campinas, Campinas, Brazil

## References

- [1] Masuda H, Fukuda K. Ordered metal nanohole arrays made by a two-step replication of honeycomb structures of anodic alumina. *Science*. 1995;268:1466–1468. DOI: 10.1126/science.268.5216.1466
- [2] Nielsch K, Muller F, Li AP, Gösele U. Uniform nickel deposition into ordered alumina pores by pulsed electrodeposition. *Advanced Materials*. 2000;12:582–586. DOI: 10.1002/(SICI)1521-4095(200004)12:8<582::AID-ADMA582>3.0.CO;2-3
- [3] Pirola KR, Navas D, Hernández-Vélez D, Nielsch K, Vázquez M. Novel magnetic materials prepared by electrodeposition techniques: arrays of nanowires and multi-layered microwires. *Journal of Applied Physics*. 2004;369:18–26. DOI: 10.1016/j.jallcom.2003.09.040
- [4] Lupu N, editor. *Electrodeposited Nanowires and their Applications*. 1st ed. Vukovar: INTECH; 2000. 236 p. DOI: 10.5772/2799



- [5] Irshad MI, Ahmad F, Mohamed NM. A Review on Nanowires as an Alternative High Density Magnetic Storage Media . In: AIP Conference Proceedings; 12–14 June 2012; Malaysia. Melville: AIP; 2012. p. 625.
- [6] Frake JC, Kano S, Ciccarelli C, Griffiths J, Sakamoto M, Teranishi T, Majima Y, Smith CG, Buitelaar MR. Radio-frequency capacitance spectroscopy of metallic nanoparticles. *Scientific Reports*. 2015;5:1–6. DOI: 10.1038/srep10858
- [7] Chena X, Wonga CKY, Yuan CA, Zhanga G. Nanowire-based gas sensors. *Sensors and Actuators B: Chemical*. 2013;177:178–195. DOI: 10.1016/j.snb.2012.10.134
- [8] Patolsky F, Zheng G, Lieber CM. Nanowire sensors for medicine and the life sciences. *Nanomedicine*. 2006;1:51–65. DOI: 10.2217/17435889.1.1.51
- [9] Moura KO, de Oliveira LAS, Rosa PFS, Béron F, Pagliuso PG, Pirola KR. Effect of dimensionality on the magnetic properties of  $\text{Fe}_3\text{Ga}_4$  crystals. *Scientific Reports*. In press.
- [10] de Oliveira LAS, Pirola KR. Synthesis, structural and magnetic characterization of highly ordered single crystalline  $\text{BiFeO}_3$  nanotubes. *Materials Research Bulletin*. 2013;48:1593–1597. DOI: 10.1016/j.materresbull.2012.12.066
- [11] Béron F, Carignan L-P, Ménard D, Yelon A. Extracting Individual Properties from Global Behaviour: First-order Reversal Curve Method Applied to Magnetic Nanowire Arrays. In: Lupu N, editor. *Electrodeposited Nanowires and their Applications*. Vukovar: INTECH; 2010. p. 167–188. DOI: 10.5772/39475
- [12] Reimer L. *Scanning Electron Microscopy: Physics of Image Formation and Microanalysis*. 2nd ed. New York: Springer; 1998. 502 p. DOI: 10.1007/978-3-540-38967-5
- [13] Oatley CW. The early history of the scanning electron microscope. *Journal of Applied Physics*. 2002;53:R1–R13. DOI: 10.1063/1.331666
- [14] Babin S, Gaevski M, Joy D, Machin M, Martynov A. Technique to automatically measure electron-beam diameter and astigmatism: BEAMETR. *Journal of Vacuum Science & Technology B*. 2006;24:2956–2959. DOI: 10.1116/1.2387158.
- [15] Utke I, Hoffmann P, Melngailis J. Gas-assisted focused electron beam and ion beam processing and fabrication. *Journal of Vacuum Science and Technology B*. 2008;26:1197–1276. DOI: 10.1116/1.2955728
- [16] Mehta R. Interactions, Imaging and Spectra in SEM. In: Kazmiruk V, editor. *Scanning Electron Microscopy*. Vukovar: INTECH; 2012. p. 17–30. DOI: 10.5772/35586
- [17] Cheng W, Steinhart M, Gosele U, Wehrspohn RB. Tree-like alumina nanopores generated in a non-steady-state anodization. *Journal of Materials Chemistry*. 2007;17:3493–3495. DOI: 10.1039/B709618F

- [18] Chen Q, Wang S, Peng LM. Establishing ohmic contacts for in situ current–voltage characteristic measurements on a carbon nanotube inside the scanning electron microscope. *Nanotechnology*. 2006;17:1087–1098. DOI: 10.1088/0957-4484/17/4/041
- [19] Hirsch P, Kässens M, Püttmann M, Reimer L. Contamination in a scanning electron microscope and the influence of specimen cooling. *Scanning*. 1994;16:101–110. DOI: 10.1002/sca.4950160207
- [20] Arzuza LCC, López-Ruiz R, Salazar-Aravena D, Knobel M, Béron F, Pirola KR. Domain wall propagation tuning in magnetic nanowires through geometric modulation. *Physical Review B*. Forthcoming.
- [21] Puydinger dos Santos MV, Lima LPB, Mayer RA, Bettini J, Béron F, Pirola K, Diniz JA. Electrical Characterization of Electrodeposited Ni Nanowires for MagFET Application. In: 30th Symposium on Microelectronics Technology and Devices (SBMicro); 31 August–4 September 2015; Salvador. New York: IEEE; 2015. p. 4. DOI: 10.1109/SBMicro.2015.7298149
- [22] Williams DB, Carter CB. *Transmission Electron Microscopy – A Textbook for Materials Science*. 2nd ed. New York: Springer; 2009. 757 p. DOI: 10.1007/978-0-387-76501-3
- [23] Reimer L, Kohl H. *Transmission Electron Microscopy*. 5th ed. New York: Springer; 2008. 590 p. DOI: 10.1007/978-0-387-40093-8
- [24] Ayache J, Beaunier L, Boumendil J, Ehret G, Laub D. *Sample Preparation Handbook for Transmission Electron Microscopy: Methodology*. 1st ed. New York: Springer; 2010. 250 p. DOI: 10.1007/978-0-387-98182-6
- [25] Kim, KH, Akase Z, Suzuki T, Shindo D. Charging effects on SEM/SIM contrast of metal/insulator system in various metallic coating conditions. *Materials Transactions*. 2010;51:1080–1083. DOI: 10.2320/matertrans.M2010034
- [26] Li, S. Nanoscale Chemical Analysis in Various Interfaces with Energy Dispersive X-ray Spectroscopy and Transmission Electron Microscopy. In: Sharma SK, editor. *X-ray Spectroscopy*. Vukovar: INTECH; 2012. p. 265–280. DOI: 10.5772/31645
- [27] Zhang J, Ma H, Zhang S, Zhang H, Deng X, Lan Q, Xue D, Bai F, Mellorsc NJ, Peng Y. Nanoscale characterisation and magnetic properties of Co<sub>81</sub>Cu<sub>19</sub>/Cu multilayer nanowires. *Journal of Materials Chemistry C*. 2015;3:85–93. DOI: 10.1039/c4tc01510j
- [28] Puydinger dos Santos MV, Velo M, Domingos RD, Bettini J, Diniz JA, Béron F, Pirola KR. Electrodeposited nickel nanowires for magnetic-field effect transistor (MagFET). *Journal of Integrated Circuits and Systems*. In press.
- [29] Rivière JC, Myhra S, editors. *Handbook of Surface and Interface Analysis Methods for Problems-solving*. 2nd ed. New York: CRC Press; 2009. 671 p.
- [30] Egerton RF. *Electron Energy-loss Spectroscopy in the Electron Microscope*. 3rd ed. New York: Springer; 2011. 491 p. DOI: 10.1007/978-1-4419-9583-4

- [31] Brydson R. *Electron Energy Loss Spectroscopy*. 1st ed. New York: Garland Science; 2001. 152 p.
- [32] Tinkov V. Non-destructive Surface Analysis by Low Energy Electron Loss Spectroscopy. In: Farrukh MA, editor. *Advanced Aspects of Spectroscopy*. Vukovar: INTECH; 2012. p. 195–220. DOI: 10.5772/48090
- [33] Maaz K, Karim S, Usman M, Mumtaz A, Liu J, Duan JL, Maqbool M. Effect of crystallographic texture on magnetic characteristics of cobalt nanowires. *Nanoscale Research Letters*. 2010;5:1111–1117. DOI: 10.1007/s11671-010-9610-5
- [34] Pirola KR, Béron F, Zanchet D, Rocha TCR, Navas D, Torrejón J, Vazquez M, Knobel M. Magnetic and structural properties fcc/hcp bi-crystalline multilayer Co nanowires array prepared by controlled electroplating. *Journal of Applied Physics*. 2011;109:083919-1–083919-6. DOI: 10.1063/1.3553865
- [35] Romeu D, Gomez A, Reyes-Gasga J. Electron Diffraction and HRTEM Structure Analysis of Nanowires. In: Hashim A, editor. *Nanowires – Fundamental Research*. Vukovar: INTECH; 2011. p. 461–484. DOI: 10.5772/18915
- [36] Chaplot SL, Mittal R, Choudhury N, editors. *Thermodynamic Properties of Solids: Experiments and Modeling*. Chichester: Wiley; 2010. 342 p. DOI: 10.1002/9783527630417.ch1
- [37] Rosa PFS, Oliveira LAS, Jesus CBR, Moura KO, Adriano C, Iwamoto W, Garitezi TM, Granada E, Saleta ME, Pirola KR, Pagliuso PG. Exploring the effects of dimensionality on the magnetic properties of intermetallic nanowires. *Solid State Communications*. 2014;191:14–18. DOI:10.1016/j.ssc.2014.04.013
- [38] Puydinger dos Santos MV, Lima LPB, Mayer RA, Béron F, Pirola K, Diniz JA. Dielectrophoretic manipulation of individual nickel nanowires for electrical transport measurements. *Journal of Vacuum Science and Technology B*. 2015;33:031804. DOI: 10.1116/1.4918732
- [39] Wu J, Yin B, Wu F, Myung Y, Banerjee P. Charge transport in single CuO nanowires. *Applied Physics Letters*. 2014;105:183506. DOI: 10.1063/1.4900966
- [40] Piroux L, Renand K, Guillemet, Mátéfi-Tempfli S, Mátéfi-Tempfli M, Antohe VA, Fusil S, Bouzheouane K, Cros V. Template-grown NiFW/Cu/NiFe nanowires for spin transfer devices. *Nano Letters*. 2007; 7:2563. DOI: 10.1021/nl070263s
- [41] Leitão DC, Sousa CT, Ventura J, Amaral JS, Carpinteiro F, Pirola KR, Vazquez M, Sousa JB, Araujo JP. Characterization of electrodeposited Ni and Ni<sub>80</sub>Fe<sub>20</sub> nanowires. *Journal of Non-Crystalline Solids*. 2008;354:5241. DOI: 10.1016/j.jnoncrysol.2008.05.088
- [42] Fusil S, Piroux L, Mátéfi-Tempfli S, Mátéfi-Tempfli M, Michotte S, Saul C K, Pereira LG, Bouzheouane K, Cros V, Deranlot C. Nanolithography based contacting method for electrical measurements on single template synthesized nanowires. *Nanotechnology*. 2005;16:2936. DOI: 10.1088/0957-4484/16/12/036

- [43] Pirola KR, Navas D, Hernández-Vélez M, Nielsch K, Vázquez M. Novel magnetic materials prepared by electrodeposition techniques: arrays of nanowires and multi-layered microwires. *Journal of Alloys and Compounds*. 2004;369:18. DOI: 10.1016/j.jallcom.2003.09.040
- [44] Ohgai T. Magnetoresistance of Nanowires Electrodeposited into Anodized Aluminum Oxide Nanochannels. In: Peng X, editor. *Nanotechnology and Nanomaterials*. Vukovar: INTECH; 2012. p. 101–125. DOI: 10.5772/52606
- [45] Vila L, Piraux L, George JM, Fert A, Faini G. Multiprobe magnetoresistance measurements on isolated magnetic nanowires. *Applied Physics Letters*. 2002;80:3805–3807. DOI: 10.1063/1.1478783
- [46] Foner S. Versatile and sensitive vibrating-sample magnetometer. *Review of Scientific Instruments*. 1959;30:548–557. DOI: 10.1063/1.1716679
- [47] Ramasamy N, Janawadkar M. SQUID Based Nondestructive Evaluation. In: Omar M, editor. *Nondestructive Testing Methods and New Applications*. Vukovar: INTECH; 2012. p. 25–52. DOI: 10.5772/36406
- [48] De La Torre Medina J, Darques M, Piraux L, Encinas A. Application of the anisotropy field distribution method to arrays of magnetic nanowires. *Journal of Applied Physics*. 2009;105:023909. DOI: 10.1063/1.3067773
- [49] Vega V, Böhnert T, Martens S, Waleczek M, Montero-Moreno JM, Görlitz D, Prida VM, Nielsch K. Tuning the magnetic anisotropy of Co-Ni nanowires: comparison between single nanowires and nanowire arrays in hard-anodic aluminum oxide membranes. *Nanotechnology*. 2012;23:465709. DOI: 10.1088/0957-4484/23/46/465709
- [50] Doudin B, Mailly D, Hasselbach K, Benoit A, Meier J, Ansermet J-P, Barbara B, Wernsdorfer W. Nucleation of magnetization reversal in individual nanosized nickel wires. *Physical Review Letters*. 1996;77:1873. DOI: 10.1103/PhysRevLett.77.1873
- [51] Tiwari U, Ghosh R, Sen P. Theory of magneto-optic Kerr effects. *Physical Review B*. 1994;49:2159. DOI: 10.1103/PhysRevB.49.2159
- [52] Mayergoyz ID. Mathematical models of hysteresis. *Physical Review Letters*. 1986;56:1518. DOI:10.1103/PhysRevLett.56.1518
- [53] Béron F, Ménard D, Yelon A. First-order reversal curve diagrams of magnetic entities with mean interaction field: a physical analysis perspective. *Journal of Applied Physics*. 2008;103:07D908. DOI: 10.1063/1.2830955
- [54] Béron F, Clime L, Ciureanu M, Ménard D, Cochrane RW, Yelon A. Magnetostatic interactions and coercivities of ferromagnetic soft nanowires in uniform length arrays. *Journal of Nanoscience and Nanotechnology*. 2008;8:2944–2954. DOI: 10.1166/jnn.2008.159

- [55] Béron F, Clime L, Ciureanu M, Ménard D, Cochrane RW, Yelon A. Reversible and quasireversible information in first-order reversal curve diagrams. *Journal of Applied Physics*. 2007;101:09J107. DOI: 10.1063/1.2712172
- [56] Dobrotă CU, Stancu A. Tracking the individual magnetic wires' switchings in ferromagnetic nanowire arrays using the first-order reversal curves (FORC) diagram method. *Physica B: Condensed Matter*. 2015;457:280–286. DOI: 10.1016/j.physb.2014.10.006
- [57] Escrig J, Lavín R, Palma JL, Denardin JC, Altbir D, Cortés A, Gómez H. Geometry dependence of coercivity in Ni nanowire arrays. *Nanotechnology*. 2008;19:07513. DOI: 10.1088/0957-4484/19/7/07513
- [58] Vivas LG, Escrig J, Trabada DG, Badini-Confaloni GA, Vázquez M. Magnetic anisotropy in ordered textured Co nanowires. *Applied Physics Letters*. 2012;100:252405. DOI: 10.1063/1.4729782
- [59] Wieser R, Vedmedenko EY, Weinberger P, Wiesendanger R. Current-driven domain wall motion in cylindrical nanowires. *Physical Review B*. 2010;82:144430. DOI: 10.1103/PhysRevB.82.144430
- [60] Yan M, Kákay A, Gliga S, Hertel R. Beating the walker limit with massless domain walls in cylindrical nanowires. *Physical Review Letters*. 2010;104:057201. DOI: 10.1103/PhysRevLett.104.057201
- [61] Ferri FA, Pereira da Silva MA, Marega Jr E. *Magnetic Force Microscopy: Basic Principles and Applications*. In: Bellitto V, editor. *Atomic Force Microscopy – Imaging, Measuring and Manipulating Surfaces at the Atomic Scale*. Vukovar: INTECH; 2012. p. 39–56. DOI: 10.5772/34833
- [62] Tabasum MR, Zighem F, De La Torre Medina J, Piroux L, Nysten B. Intrinsic switching field distribution of arrays of Ni<sub>80</sub>Fe<sub>20</sub> nanowires probed by in situ magnetic force microscopy. *Journal of Superconductivity and Novel Magnetism*. 2013;26:1375–1379. DOI: 10.1007/s10948-012-1975-5
- [63] Yuana J, Peia W, Hasagawaa T, Washiyaa T, Saitoa H, Ishioa S, Oshimac H, Itoh K. Study on magnetization reversal of cobalt nanowire arrays by magnetic force microscopy. *Journal of Magnetism and Magnetic Materials*. 2008;320:736–741. DOI: 10.1016/j.jmmm.2007.08.023
- [64] Ebels U, Radulescu A, Henry Y, Piroux L, Ounadjela K. Spin Accumulation and domain wall magnetoresistance in 35 nm Co wires. *Physical Review Letters*. 2000;84:983–986. DOI:10.1103/PhysRevLett.84.983
- [65] Vázquez M, Hernández-Vélez M, Pirola K, Asenjo A, Navas D, Velázquez J, Vargas P, Ramos C. Arrays of Ni nanowires in alumina membranes: magnetic properties and spatial ordering. *The European Physical Journal B*. 2004;40:489–497. DOI: 10.1140/epjb/e2004-00163-4

- [66] Akhtari-Zavareh A, Carignan LP, Yelon A, Ménard D, Kasama T, Herring R, Dunin-Borkowski RE, McCartney MR, Kavanagh KL. Off-axis electron holography of ferromagnetic multilayer nanowires. *Journal of Applied Physics*. 2014;116:023902. DOI: 10.1063/1.4887488
- [67] Tonomura A. Fundamentals and Applications of Electron Holography. In: Rosen J, editor. *Holography, Research and Technologies*. Vukovar: INTECH; 2011. p. 441–452. DOI: 10.5772/14280
- [68] Kasama T, Dunin-Borkowski RE, Beleggia M. Electron Holography of Magnetic Materials. In: Monroy Ramirez FA, editor. *Holography – Different Fields of Application*. Vukovar: INTECH; 2011. p. 53–80. DOI: 10.5772/22366
- [69] Biziere N, Gatel C, Lassalle-Balier R, Clochard MC, Wegrowe JE, Snoeck E. Imaging the fine structure of a magnetic domain wall in a Ni nanocylinder. *Nano Letters*. 2013;13:2053–2057. DOI: 10.1021/nl400317j
- [70] Yalcin O. Ferromagnetic Resonance. In: Yalcin O, editor. *Ferromagnetic Resonance – Theory and Applications*. Vukovar: INTECH; 2013. p. 1–46. DOI: 10.5772/56134
- [71] Carignan LP, Yelon A, Ménard D, Caloz C. Ferromagnetic Nanowire Metamaterials: Theory and Applications. *IEEE Transactions on Microwave Theory and Technique*. 2011;59:2568–2586. DOI:10.1109/TMTT.2011.2163202
- [72] Carignan LP, Boucher V, Kodera T, Caloz C, Yelon A, Ménard D. Double ferromagnetic resonance in nanowire arrays. *Applied Physics Letters*. 2009;95:062504. DOI: 10.1063/1.3194296
- [73] Sharma M, Pathak S, Monika Sharma M. FMR Measurements of Magnetic Nanostructures. In: Yalcin O, editor. *Ferromagnetic Resonance – Theory and Applications*. Vukovar: INTECH; 2013. p. 93–110. DOI: 10.5772/56615
- [74] Carignan LP, Lacroix C, Ouimet A, Ciureanu M, Yelon A, Ménard D. Magnetic anisotropy in arrays of Ni, CoFeB, and Ni/Cu nanowires. *Journal of Applied Physics*. 2007;102:023905. DOI: 10.1063/1.2756522

